Front. Optoelectron. China 2009, 2(3): 334–338
DOI 10.1007/s12200-009-0014-z

RESEARCH ARTICLE

Numerical investigation on machining glass with CO_2 lasers

Junke JIAO[1,2], Xinbing WANG (✉)[1]

1 Wuhan National Laboratory for Optoelectronics, Huazhong University of Science and Technology, Wuhan 430074, China
2 Institute of Industry Technology, Guangzhou and Chinese Academy of Sciences, Guangzhou 511458, China

Abstract When a glass substrate was irradiated by three different temporal shapes of laser sources, namely, line-time-shape laser, triangle-time-shape laser, and parabola-time-shape laser, the mathematical models were proposed, and the temperature distribution and the resulting thermal stress were calculated by the finite-element-method (FEM) software ANSYS. With these three types of lasers having the same output laser energy, the resulting thermal stress induced in the glass substrate was analyzed. The results showed that, with the same output laser energy, the thermal stress produced in glass heated by line-time-shape laser is higher than that produced in glass heated by the other two shapes of lasers.

Keywords laser machining, soda-lime glass, finite-element-method (FEM), ANSYS

1 Introduction

With the development of laser technology, many studies have been carried out on cutting glass with lasers [1–17]. Li et al. [3] put forward a mathematical model to explain the heat transfer of glass heated by a laser beam. Wei et al. [4] and Tian et al. [5] investigated the thermal behavior of glass heated by a CO_2-laser beam numerically, and concluded that the resulting temperature distribution was strongly dependent on the speed and the parameters of the laser beam. Tsai et al. [6] studied the thermal stress of alumina ceramic substrates irradiated by a moving laser beam and some experiments were carried out to investigate how the crack propagation was influenced by laser power, cutting speed, and specimen geometry.

Glass can be cut by continuous-wave lasers in two different ways. One is the controlled fracture method and the other is melting means. The former has attracted more attention and lots of research has been reported in literatures [7–16]. In contrast, very few studies have been made in detail to investigate cutting glass with the melting method except by Chui [17], due to the low thermal conductivity and the brittleness of the glass material. How to reduce the thermal stress in the glass manufacturing process is a challenging task. Thermal stress is always generated by rapid heating or cooling. If the glass is heated slowly and cools down smoothly, the thermal stress may be controlled below the critical value. In this study, three different temporal shapes of lasers were used to heat the glass substrate, and the thermal stress was calculated by using finite-element-method (FEM) software ANSYS.

Received October 13, 2008; accepted December 16, 2008

E-mail: xbwang@mail.hust.edu.cn

2 Theoretical approaches

As shown in Fig. 1, the length L, width W, and thickness H of the glass substrate are 40 mm, 20 mm, and 2 mm, respectively. A stationary unfocused CO_2-laser irradiates on the surface and the diameter of this laser beam is 6 mm. Before establishing mathematical models, some assumptions should be made as follows.

1) The physical properties of the glass material are isotropic and symmetrical.

2) There is no phase change in the machining process.

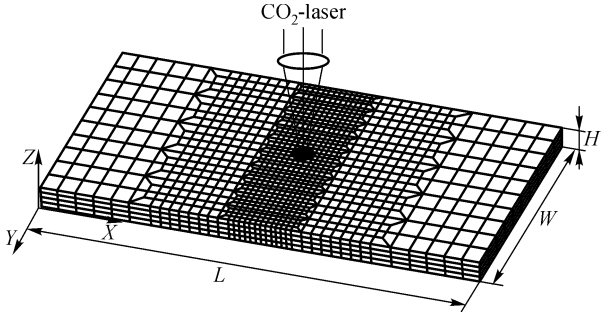

Fig. 1 Diagram of glass laser heating and grid structure of glass substrate

3) On the surface of the glass, without laser heating, the superficial heat irradiation is negligible.

4) The CO_2-laser energy is fully absorbed by soda-lime glass ($\alpha = 1$), and the emission coefficient ε is treated as 1.

2.1 Mathematical models for heat transfer and mechanism

Based on the above-mentioned assumptions, the mathematical heat transfer model can be established as follows:

$$\begin{cases} \rho c \dfrac{\partial T}{\partial t} = k\nabla^2 T, & \\ T(t) = T_0, & t = 0, \\ -k \dfrac{\partial T}{\partial z} + h(T_s - T_0) + B\varepsilon(T_s^4 - T_0^4) = \alpha I(x, y, z, t), & z = H, \\ -k \dfrac{\partial T}{\partial n} = h(T_n - T_0), & z = 0, \quad x = 0, L, \quad y = \pm \dfrac{W}{2}, \end{cases} \tag{1}$$

where k is the thermal conductivity; c and ρ are the heat capacity and the density, respectively; T_0 denotes the initial temperature of glass which is the same as the environment temperature; T_s denotes the temperature of heated zone and T_n denotes the temperature of the area without laser heating; h is the convection heat-transfer coefficient and B is the Stefan-Bolzmann constant; $I(x, y, z, t)$ is the density of the laser power and n is the direction cosine of boundary.

In this study, the stress and strain responses were assumed to be quasi-static at each interval and the thermo-elastic model was used. The entire surfaces of the glass plate are free of stress, and the distribution of the thermal stress can be obtained by solving the heat-elasticity equation mentioned in Ref. [18]. During the process of laser glass machining, the thermal stress may be established as a result of thermal gradients in glass, frequently caused by rapid heating or cooling. Here, caused by a temperature difference ΔT, the thermal stress σ_{therm} is given as [19]

$$\sigma_{\text{therm}} = \frac{E\beta\Delta T}{1-\theta}, \tag{2}$$

where θ is the Poisson's ratio, and E and β are the Yang's modulus and the coefficient of linear expansion, respectively. From Eq. (2), the sharp change in temperature will lead to a steep thermal gradient and a large thermal stress. Heating and cooling down the glass substrate smoothly may be a feasible means to reduce this thermal stress in the machining process.

2.2 Model of laser beam

Lasers focusing on the top surface maintain a constant TEM_{00} mode. The density of the laser power can be described by Gaussian distribution as

$$I(x, y, z, t) = \frac{P}{\pi r^2} \exp\left(-\frac{x^2 + y^2}{r^2}\right)\delta(z), \tag{3}$$

where P and r are the power and the radius of the CO_2-laser beam, respectively. The absorption depth is less than 15 μm, so the CO_2-laser beam is treated as a surface heating source, and an impulse function $\delta(z)$ is applied in Eq. (3).

In this study, three different temporal shapes of laser sources were used to heat the glass substrate, and the difference of the thermal behavior among them was studied to find a best temporal shape of laser to reduce the thermal stress. The output power for these three different laser sources is

$$P = \begin{cases} P_0, & 0 \leqslant t \leqslant t_0, \quad \text{line}, \\ P_0\left(1 - \dfrac{|t - t_0|}{t_0}\right), & 0 \leqslant t \leqslant 2t_0, \quad \text{triangle}, \\ \dfrac{3}{4} P_0\left[1 - \left(\dfrac{t - t_0}{t_0}\right)^2\right], & 0 \leqslant t \leqslant 2t_0, \quad \text{parabola}. \end{cases} \tag{4}$$

In the current work, P_0= 30 W and t_0= 10 s. The output power temporal histories for these three shapes of laser sources are shown in Fig. 2. For the line-time-shape laser, the output power keeps in a constant value (P = 30 W) in the first 10 s, and there is no output laser in the next 10 s. For triangle-time-shape laser source and parabola-time-shape laser source, the power of the laser increases in the

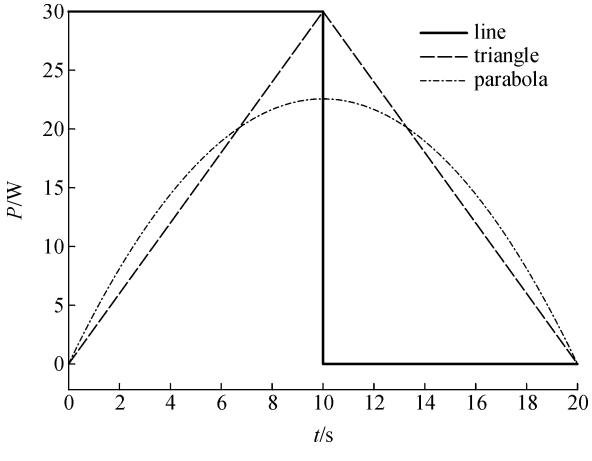

Fig. 2 Time history of power for line-time-shape, triangle-time-shape, and parabola-time-shape lasers

first 10 s, and decreases slowly in the following 10 s. It should be noted that the output laser energy is the same for these three temporal shapes of laser sources during the analyzing time (0–20 s).

3 Numerical calculations

A coupled-field analysis was performed to determine the temperature distribution and the resulting thermal stress in the workpiece using the FEM software ANSYS. The coupling between the thermal and structural fields was accomplished by direct coupling. A three-dimensional coupled-field solid element in SOLID5 was used for the current work. The element had eight nodes with up to six degrees of freedom at each node. The grid structure of the glass substrate is shown in Fig. 1. On the heated zone, the size of elements is optimized balancing the demand for simulating precision and computational efficiency, which turns out to be smaller than that in other regions. The size of elements on the heated zone is 0.5 mm, which is accurate enough for this study.

The physical parameters of soda-lime glass are shown in Table 1 [11]. The initial temperature T_0 was 20°C and the convection heat-transfer coefficient h was 10 $W \cdot m^{-2} \cdot K^{-1}$.

4 Results and discussion

According to the above-mentioned mathematical models and the parameters of the soda-lime glass given in Table 1, the distribution of the temperature and the resulting thermal stress can be calculated by using the FEM software ANSYS, which is powerful in coupling thermal and structural fields.

When the glass substrate is irradiated by these three temporal shapes of laser sources, the temperature history is given in Fig. 3. For line-time-shape laser, the workpiece is heated by high-density laser beam, and the temperature increases rapidly in the first 10 s. Then, the workpiece is cooled down sharply by the convection between the workpiece and the air surrounding in the following 10 s. This rapid heating and cooling will result a large thermal stress in the glass substrate. On the other hand, for triangle-time-shape and parabola-time-shape laser sources, the power increases with time slowly in the first 10 s and descends smoothly in the next 10 s. When the workpiece is irradiated by these two temporal shapes of laser sources, the temperature varies smoothly, and the thermal gradient and the resulting thermal stress would be very small.

With these three temporal shapes of lasers having the same output laser energy, the maximum value of the temperature generated in the glass substrate is different. The maximum temperature for line-time-shape laser is much higher than the other two laser sources due to the low thermal conductivity of the glass material, and the heat energy is accumulated on the heating zone at a short time for line-time-shape laser. Otherwise, the maximum temperature is a little higher for triangle-time-shape laser than that for parabola-time-shape laser.

In the heating zone, because of the high temperature, a compressive thermal stress is generated (see Fig. 4). The resulting compressive thermal stress is higher for line-time-shape laser than that for the other two shapes of laser sources. The thermal stress changes most smoothly for parabola-time-shape laser and most sharply for line-time-shape laser.

At the time step $t = 10$ s, which is the inflexion of the output laser, the temperature on the top surface is much higher for line-time-shape laser than those for triangle-time-shape and parabola-time-shape lasers (see Fig. 5). In the last 10 s, the tensile stress decreases with time for line-time-shape laser, and the minimum value is 140 MPa at the time step $t = 20$ s at the edge of the glass substrate (see Fig. 6). However, for triangle-time-shape and parabola-time-shape lasers, the tensile stress reaches to the maximum value at the time step $t = 14$ s and then decreases to 178 MPa (see Fig. 7) and 175 MPa (see Fig. 8) at the time step $t = 20$ s, respectively.

When a laser beam is irradiating on glass substrate, the maximum tensile stress occurs at the edge of the workpiece. This tensile stress is an important factor in glass laser machining. If this stress exceeds the critical value, a fracture will be produced. In glass laser cutting with the controlled fracture method, this fracture propagates in a predicted way to separate the glass substrate. However, in most glass manufacturing processes, this tensile stress is negative, such as cutting glass in the melting method and shaping glass materials. In these machining processes, the tensile stress is a negative factor that has to be reduced.

Table 1 Physical properties of soda-lime glass

T/°C	20	200	400	600	800	1000
ρ/($kg \cdot m^{-3}$)	2520	—	—	—	—	—
β	8.7×10^{-6}	—	—	—	—	—
k/($W \cdot K^{-1}$)	1.40	1.62	1.82	2.10	—	—
c/[$J \cdot (kg \cdot K)^{-1}$]	680	955	1075	1145	1195	1220
θ	0.165	0.173	0.177	0.182	0.186	0.194
E/GPa	72.9	75.0	77.2	78.8	80.0	81.0

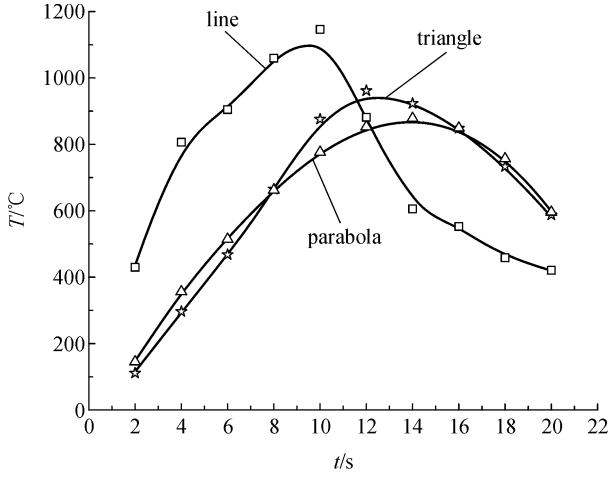

Fig. 3 Temperature history in laser heating zone

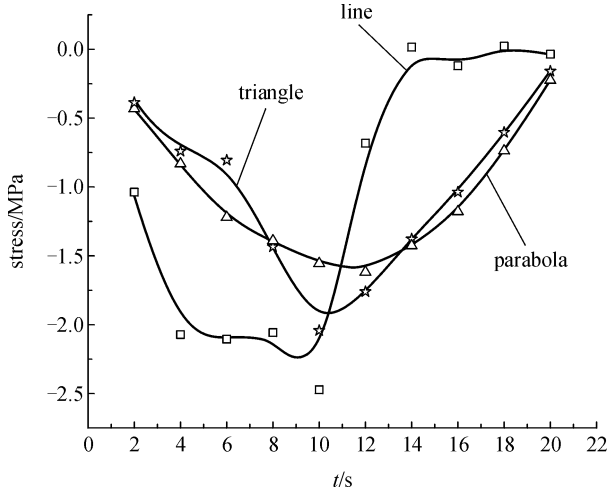

Fig. 4 Thermal stress history in laser heating zone

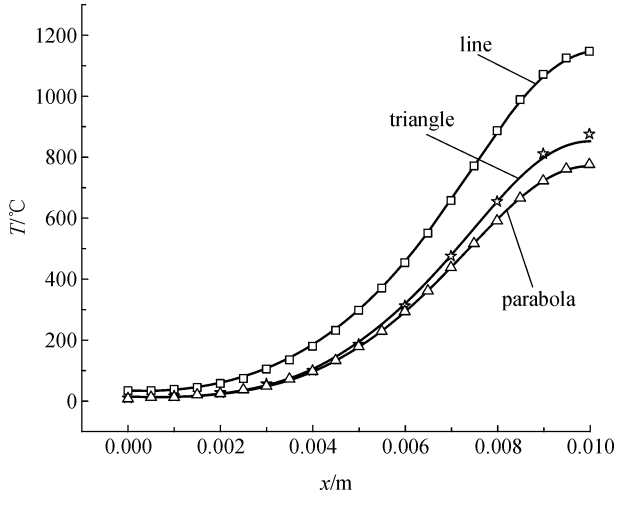

Fig. 5 Temperature distribution on heating surface at time step $t = 10$ s

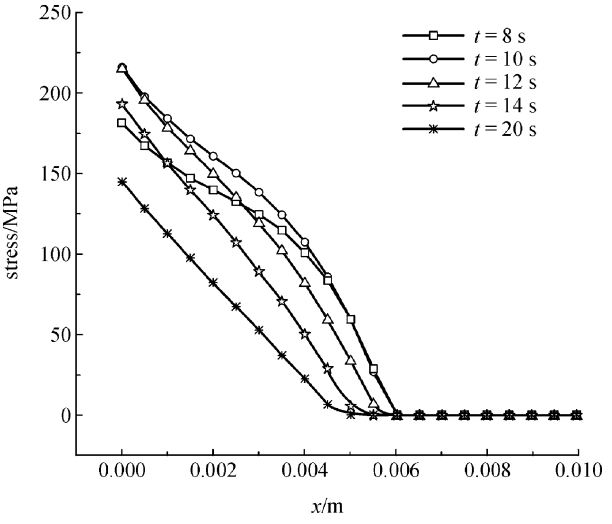

Fig. 6 Thermal stress on heating surface at different time for line-time-shape laser

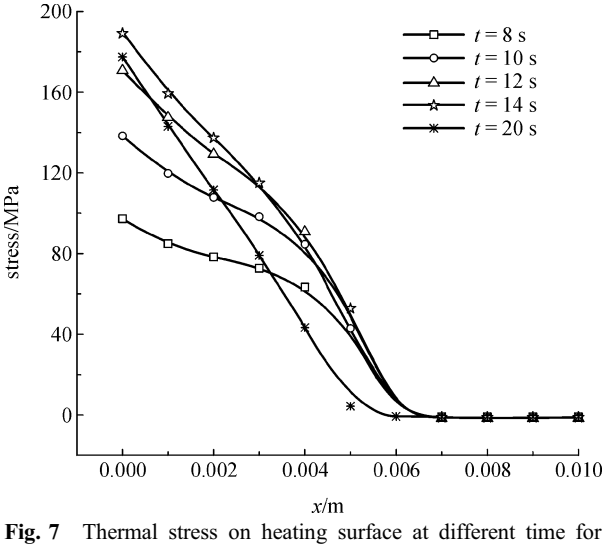

Fig. 7 Thermal stress on heating surface at different time for triangle-time-shape laser

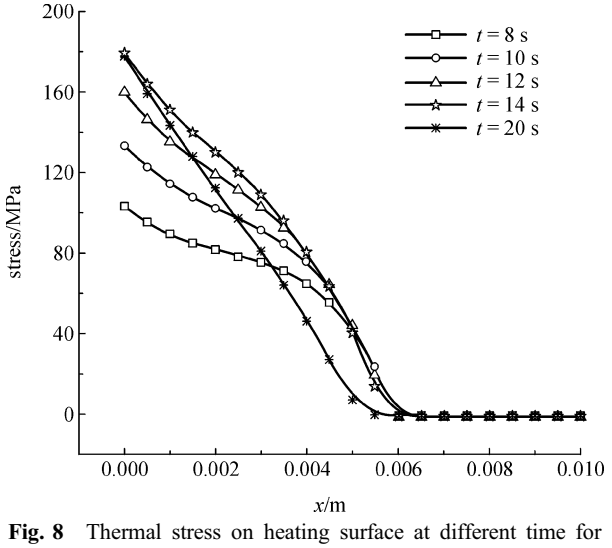

Fig. 8 Thermal stress on heating surface at different time for parabola-time-shape laser

For line-time-shape laser, the maximum tensile stress occurs at the time step $t = 10$ s (see Fig. 6), which is the point of the laser stopping to irradiate the glass. On the other hand, for triangle-time-shape and parabola-time-shape lasers, the maximum tensile stress occurs at the time step $t = 14$ s (see Figs. 7 and 8). This phenomenon is consistent with the temperature history for these two laser sources. On the other hand, the maximum tensile stress is much larger for line-time-shape laser than that for triangle-time-shape and parabola-time-shape lasers with the same output laser energy.

5 Conclusion

The mathematical models of glass irradiated by line-time-shape, triangle-time-shape, and parabola-time-shape lasers were put forward. The temperature distribution and the resulting thermal stress were calculated by ANSYS. For line-time-shape laser, the workpiece was heated to a high temperature in a short time and cooled down rapidly in the air surrounding. And, a higher thermal stress including the compressive stress in the heating zone and the tensile stress at the edge of glass substrate were generated. For triangle-time-shape and parabola-time-shape lasers, the workpiece was heated slowly in the first 10 s and cooled down smoothly in the following 10 s. And, the temperature varied more smoothly and a smaller thermal stress was generated in the machining process.

Acknowledgements This work was supported by the National Natural Science Foundation of China (Grant No. 60478028).

References

1. Kang H S, Hong S K, Oh S C, Choi J Y, Song M G. A study of cutting glass by laser. Proceedings of SPIE, 2002, 4426: 367–370
2. Hermanns C. Laser cutting of glass. Proceedings of SPIE, 2000, 4102: 219–226
3. Li J F, Li L, Stott F H. Comparison of volumetric and surface heating sources in the modeling of laser melting of ceramic materials. International Journal of Heat and Mass Transfer, 2004, 47 (6–7): 1159–1174
4. Wei C Y, He H B, Deng Z, Shao J D, Fan Z X. Study of thermal behaviors in CO_2 laser irradiated glass. Optical Engineering, 2005, 44(4): 044202-1–044202-4
5. Tian W X, Chiu K S. Temperature prediction for CO_2 laser heating of moving glass rods. Optics and Laser Technology, 2004, 36(2): 131–137
6. Tsai C H, Liou C S. Fracture mechanism of laser cutting with controlled fracture. Journal of Manufacturing Science and Engineering, 2003, 125(3): 519–528
7. Lumley M R. Controlled separation of brittle materials using a laser. American Ceramic Society Bulletin, 1969, 48(9): 850–854
8. Tsai C H, Chen C J. Formation of the breaking surface of alumina in laser cutting with a controlled fracture technique. Proceedings of the Institution of Mechanical Engineers, Part B: Journal of Engineering Manufacture, 2003, 217(4): 489–497
9. Tsai C H, Lin B C. Laser cutting with controlled fracture and pre-bending applied to LCD glass separation. International Journal of Advanced Manufacturing Technology, 2007, 32(11–12): 1155–1162
10. Zheng H Y, Lee T. Studies of CO_2 laser peeling of glass substrates. Journal of Micromechanics and Microengineering, 2005, 15(11): 2093–2097
11. Wang Y Z, Lin J. Characterization of the laser cleaving on glass sheets with a line-shape laser beam. Optics and Laser Technology, 2007, 39(5): 892–899
12. Zhou B H, Mahdavian S M. Experimental and theoretical analyses of cutting nonmetallic materials by low power CO_2-laser. Journal of Materials Processing Technology, 2004, 146(2): 188–192
13. Brugan P, Cai G, Akarapu R, Segall A E. Controlled-fracture of prescored alumina ceramics using simultaneous CO_2 lasers. Journal of Laser Applications, 2006, 18(3): 236–241
14. Santiago V P, Washington M, Brugan P, Cai G, Akarapu R, Pulford S, Segall A E. Faster and damage-reduced laser cutting of thick ceramics using a simultaneous prescore approach. Journal of Laser Applications, 2005, 17(4): 219–224
15. Abrams M B, Green D J, Glass S J. Fracture behavior of engineered stress profile soda lime silicate glass. Journal of Non-crystalline Solids, 2003, 321(1–2): 10–19
16. Wiederhorn S M, Dretzke A, Rödel J. Crack growth in soda-lime-silicate glass near the static fatigue limit. Journal of the American Ceramics Society, 2002, 85(9): 2287–2292
17. Chui G K. Laser cutting of hot glass. American Ceramic Society Bulletin, 1975, 54(5): 514–518
18. Akarapu R, Segall A E. Numerical simulations of an active-stressing technique for delaying fracture during cutting of alumina. Journal of Manufacturing Science and Engineering, 2006, 128(4): 921–927
19. Triantafyllidis D, Bernstein J R, Li L, Stott F H. Dual laser beam modification of high alumina ceramics. Journal of Laser Applications, 2003, 15(1): 49–54